doi:10.1016/j.jmb.2004.05.072 *J. Mol. Biol.* (2004) **341**, 605–615

JMB

Available online at www.sciencedirect.com

SCIENCE DIRECT®

ELSEVIER

Iron Binding and Oxidation Kinetics in Frataxin CyaY of *Escherichia coli*

Fadi Bou-Abdallah[1], Salvatore Adinolfi[2], Annalisa Pastore[2] Thomas M. Laue[3] and N. Dennis Chasteen[1]*

[1]*Department of Chemistry University of New Hampshire Durham, NH 03824, USA*

[2]*National Institute for Medical Research, The Ridgeway-London NW7 1AA UK*

[3]*Center to Advance Molecular Interaction Science, CAMIS University of New Hampshire Durham, NH 03824, USA*

**Corresponding author*

Friedreich's ataxia is associated with a deficiency in frataxin, a conserved mitochondrial protein of unknown function. Here, we investigate the iron binding and oxidation chemistry of *Escherichia coli* frataxin (CyaY), a homologue of human frataxin, with the aim of better understanding the functional properties of this protein. Anaerobic isothermal titration calorimetry (ITC) demonstrates that at least two ferrous ions bind specifically but relatively weakly per CyaY monomer ($K_d \sim 4$ μM). Such weak binding is consistent with the hypothesis that the protein functions as an iron chaperone. The bound Fe(II) is oxidized slowly by O_2. However, oxidation occurs rapidly and completely with H_2O_2 through a non-enzymatic process with a stoichiometry of two Fe(II)/H_2O_2, indicating complete reduction of H_2O_2 to H_2O. In accord with this stoichiometry, electron paramagnetic resonance (EPR) spin trapping experiments indicate that iron catalyzed production of hydroxyl radical from Fenton chemistry is greatly attenuated in the presence of CyaY. The Fe(III) produced from oxidation of Fe(II) by H_2O_2 binds to the protein with a stoichiometry of six Fe(III)/CyaY monomer as independently measured by kinetic, UV–visible, fluorescence, iron analysis and pH-stat titrations. However, as many as 25–26 Fe(III)/monomer can bind to the protein, exhibiting UV absorption properties similar to those of hydrolyzed polynuclear Fe(III) species. Analytical ultracentrifugation measurements indicate that a tetramer is formed when Fe(II) is added anaerobically to the protein; multiple protein aggregates are formed upon oxidation of the bound Fe(II). The observed iron oxidation and binding properties of frataxin CyaY may afford the mitochondria protection against iron-induced oxidative damage.

© 2004 Elsevier Ltd. All rights reserved.

Keywords: frataxin; iron toxicity; iron metabolism; radicals; isothermal titration calorimetry

Introduction

The continuous supply of iron to the mitochondria is an important requirement for the biosynthesis of heme and iron–sulfur clusters.[1,2] Maintaining the mitochondrial iron pool in a soluble and bio-available form is a constant challenge for all living cells. Under physiological conditions, mononuclear Fe(II) can be rapidly oxidized to insoluble Fe(III), either by dioxygen to generate superoxide radical or by hydrogen peroxide, a by-product of respiration, to produce hydroxyl radical, the most reactive of oxygen species. Therefore, the need for highly efficient iron transport, storage, and detoxification systems is important to overcome the dual paradox imposed by iron, namely its poor solubility/bioavailability and toxicity.

Almost three decades ago, Flatmark & Romslo reported the presence of "non-heme non-iron–sulfur" iron inside the matrix of isolated rat liver

Abbreviations used: CyaY, bacterial frataxin; Dps, DNA binding protein from starved cells; DTPA, diethylenetriamine pentaacetic acid; EcBFR, *E. coli* bacterioferritin; IAA, iodoacetamide; EMPO, 5-ethoxycarbonyl-5-methyl-1-pyrroline-*N*-oxide; EPR, electron paramagnetic resonance; ITC, isothermal titration calorimetry; Mops, 3-(*N*-morpholino) propanesulfonic acid.

E-mail address of the corresponding author: ndc@cisunix.unh.edu

0022-2836/$ - see front matter © 2004 Elsevier Ltd. All rights reserved.

mitochondria and suggested that a macromolecule distinct from ferritin might be responsible for the soluble and stable form of iron inside the mitochondria.[3] Recently, several mitochondrial proteins have been identified within the mitochondria and proven to be involved in mitochondrial iron transport.[4–6]

Frataxin, a protein implicated in iron metabolism[7–10] was first identified as the mitochondrial protein deficient in Friedreich's ataxia (FRDA), an autosomal recessive cardio and neurodegenerative disease.[11,12] It is a 210 amino acid pre-proprotein that is targeted to the mitochondrial matrix and found highly concentrated in the cells of heart, spinal cord and dorsal root ganglia, an expression that explains its correlation with neural degeneration, cardiomyopathy and increased risk of diabetes.[13]

Frataxin has poor amino acid sequence homology with other known proteins involved in iron or heme metabolism and its precise biological function remains unclear.[12–14] However, frataxin appears to be important for maintaining overall cellular iron homeostasis and for minimizing iron-induced oxidative reactions. More recently, ferroxidase activity for both yeast and human frataxin has been reported and a mineral core similar to the hydrous ferric oxide mineral found in ferritins has been identified by X-ray absorption spectroscopy in both proteins.[15–17]

Accordingly, and because of the apparent involvement of frataxin in normal cellular iron homeostasis, it has been suggested that the basic function of frataxin is to provide an iron storage mechanism similar to that of ferritin in order to keep iron in a bio-available and non-toxic form.[2,15,18,19] However, recent studies point to a role of frataxin as an iron chaperone for iron–sulfur cluster (Isc) and heme biosyntheses.[20–25]

To characterize further the functions of frataxin, it is necessary to develop suitable model systems which can be used both for *in vitro* and *in vivo* studies. We have recently demonstrated that CyaY, the bacterial homologue of frataxin, is an excellent candidate, since it does not contain the import signal typical of the eukaryotic species and is well folded and thermodynamically stable.[26] A bacterial model system is advantageous also because several Isc proteins from *Escherichia coli* and other bacteria are well characterized. Here, we present a careful investigation of iron binding properties of *E. coli* CyaY and the influence of iron on the protein self-assembly. We demonstrate that CyaY forms multiple aggregates in the presence of Fe(III) but the assembly appears to be a non-specific process. CyaY binds specifically, but relatively weakly, two ferrous ions whereas the protein can accommodate six or more ferric ions. We also provide a detailed account of the oxidation and hydrolysis chemistry of the protein and compare its properties with those of ferritins, demonstrating that CyaY and the ferritins have distinct features.

Results

Iron oxidation kinetics

The kinetics of Fe(II) oxidation with CyaY using O_2 and H_2O_2 as oxidants were initially examined. The rate of iron(II) oxidation in the presence and absence of CyaY was followed by the absorbance change at 305 nm due to the formation of oxo/hydroxo Fe(III) species (Figure 1(a)). In these experiments, an Fe(II)/protein ratio of 6/1 was employed which corresponds to the measured Fe(III) binding stoichiometry (see below). Figure 1(a) shows the kinetic profile of Fe(II) oxidation in the presence of frataxin (curve (E)) *versus* buffer alone (curve (D)) using O_2 as the oxidant. The rate of iron oxidation in buffer alone is twice as fast as the rate when CyaY is present, indicating that the protein itself retards Fe(II) oxidation ($v = 1.32 \times 10^{-4}\ s^{-1}$ *versus* $0.79 \times 10^{-4}\ s^{-1}$ measured over the first six minutes of the reaction). Spectrophotometric measurement of the unreacted Fe(II) over the same time interval using the ferrous

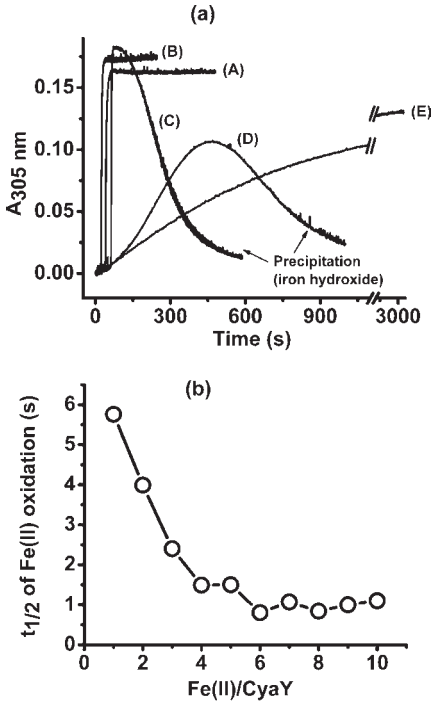

Figure 1. (a), Spectrophotometric kinetic curves of Fe(II) oxidation by H_2O_2 in CyaY (A), egg albumin (B), and in buffer alone (C), and Fe(II) oxidation by O_2 in CyaY (E) and in buffer alone (D). (b), Half-life of Fe(II) oxidation by H_2O_2 as a function of Fe(II) added to the protein. Conditions for (a): 10 μM CyaY or 3 μM egg albumin, 60 μM $FeSO_4$, 120 μM H_2O_2 or 21% O_2, 50 mM Mops, 150 mM NaCl (pH 7.50). Kinetics were monitored at 305 nm and 25 °C. Conditions for (b): 30.5 μM CyaY, 50 mM Mops, 150 mM NaCl (pH 7.0). One Fe(II)/CyaY was added to the same anaerobic protein solution followed by 0.5 H_2O_2/Fe(II) each time. Kinetics were monitored at 295 nm and 25 °C.

chelator Ferrozine confirmed that the rate is twofold slower for CyaY compared to buffer. In contrast, when H_2O_2 was employed as the oxidant (Figure 1(a), curve (A)), the reaction in the presence of CyaY was rapid and complete, being ~670 times faster ($v = 0.053\ s^{-1}$) than with O_2 ($v = 0.79 \times 10^{-4}\ s^{-1}$). A similar fast rate was observed in a control experiment with egg albumin and H_2O_2 (curve (B)) but, as demonstrated below, CyaY greatly attenuates radical formation whereas albumin does not. As expected, Fe(II) oxidation by H_2O_2 in buffer in the absence of either protein also occurs rapidly (curve (C)) but precipitation of ferric hydroxide occurs as also found with O_2 as the oxidant (curve (D)).

Subsequent experiments largely focused on the use of H_2O_2, since it is the most efficient oxidant for Fe(II) in CyaY. Kinetic measurements were carried out to determine the dependence of the rate of Fe(II) oxidation on the amount of iron added to the protein. The sequential addition of increments of one Fe(II)/CyaY to the same anaerobic protein sample followed by the addition of 0.5 H_2O_2/Fe(II) each time (an amount sufficient to oxidize all the iron, see below) resulted in a progressively faster rate of Fe(II) oxidation. The half-life for Fe(II) oxidation reached a minimum at a total of ~6 Fe(II)/CyaY added, remaining constant thereafter as shown in Figure 1(b). These results demonstrate that CyaY lacks enzymatic activity toward Fe(II) oxidation, otherwise the same half-life would have been obtained for each Fe(II) addition as typical of a catalytic process. Rather, the data show a changing rate of oxidation for the first six Fe(II) added, indicating that this first group of iron has distinct reaction properties from the iron added subsequently.

The stoichiometry of iron(II, III) binding

Isothermal titration calorimetry (ITC) of Fe(II) binding

Anaerobic ITC binding experiments were performed to determine the number of principal sites on the protein that bind Fe(II). Figure 2(a) shows the raw ITC data for Fe(II) binding to CyaY at pH 7.0 and the integrated heats (μJ) for each injection (Figure 2(b)) *versus* the Fe(II)/apoprotein molar ratio. An exothermic reaction is seen and a good fit of the data is achieved using a model with one set of two independent binding sites with an association constant of $K = 2.6 \times 10^5\ M^{-1}$ ($K_d = 3.8\ \mu M$) (Figure 2(b)). Ultrafiltration experiments (Materials and Methods) indicate that there are additional much weaker Fe(II) binding sites on CyaY; however, the weak binding properties of these sites do not permit us to determine their stoichiometry and affinity with complete confidence (data not shown).

Spectrophotometric and pH-stat titrations of Fe(III) binding

To establish the stoichiometry of Fe(III) binding,

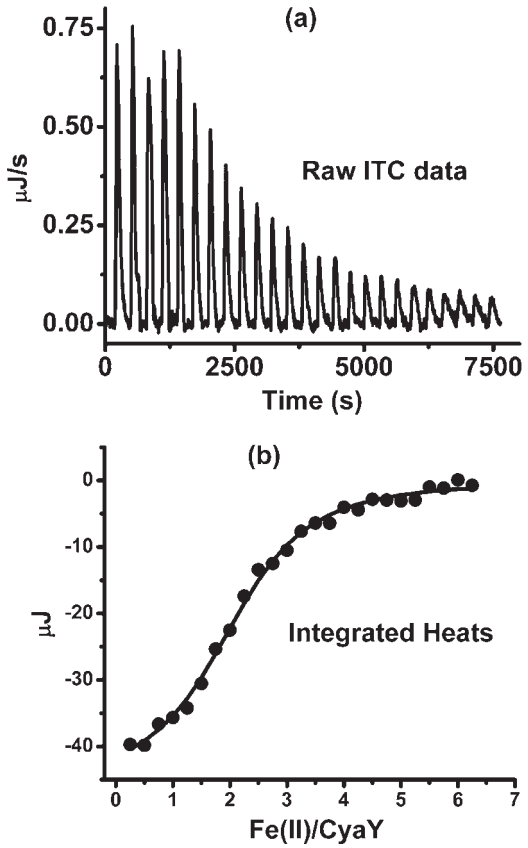

Figure 2. Calorimetric titration of the bacterial frataxin CyaY with Fe(II) under anaerobic conditions. (a), Raw data. (b), Plot of the integrated heat *versus* the Fe(II)/CyaY molar ratio. The continuous line is the fitted curve for the thermodynamic parameters: $n = 2.16$ (± 0.18); $K = 2.57$ (± 1.30) $\times 10^5\ M^{-1}$; $\Delta H^\circ = -4.88$ (± 0.30) kJ/mol; $\Delta G^\circ = -RT\ln K = -30.86$ (± 1.25) kJ/mol; $\Delta S^\circ = (\Delta H^\circ - \Delta G^\circ)/T = 87.2$ (± 4.3) J/mol. Conditions: 25 μM CyaY titrated with 10 μl injections of 0.8125 mM $FeSO_4$ in 50 mM Mops buffer, 150 mM NaCl, 2 mM $Na_2S_2O_4$ in both protein and Fe(II) solution (pH 7.0) and 25.00 °C.

UV–visible and fluorescence spectrophotometries and pH-stat measurements were carried out while titrating CyaY with iron. Figure 3 shows the UV spectral changes at 296 nm upon multiple anaerobic additions of one Fe(II)/CyaY followed by 0.5 H_2O_2/Fe(II) each time in 50 mM Mops, 200 mM NaCl (pH 7.50). Spectra characteristic of polynuclear Fe(III) oxo(hydroxo) species are produced. A discontinuity in absorbance at ~6 Fe(II)/CyaY is evident in Figure 3 (inset), indicating that an initial group of six Fe(III) associate with the protein. However, the continued rise in absorbance beyond six Fe/CyaY without precipitation indicates that additional Fe(III) binding occurs. Since previous experiments have shown an influence of the ionic strength on iron promoted aggregation,[26] a UV stoichiometric titration was also conducted with CyaY at lower ionic strength (0.1 M Mops, 50 mM NaCl (pH 7.50)). The binding

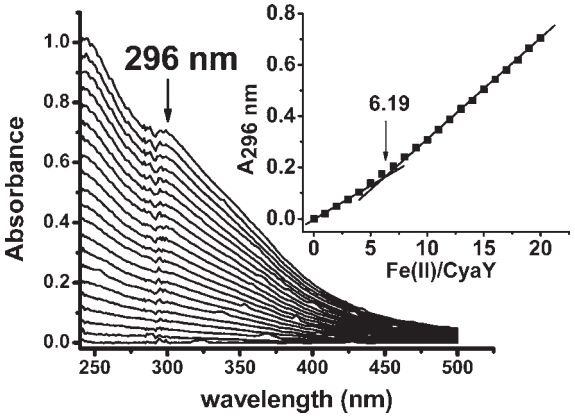

Figure 3. Spectrometric titration spectra of bacterial frataxin CyaY with Fe(II) and H_2O_2 under anaerobic conditions. Inset: titration curve for each addition of one Fe(II)/protein followed by 0.5 H_2O_2/Fe(II) per addition. Conditions: 20 μM protein, 50 mM Mops, 200 mM NaCl (pH 7.50).

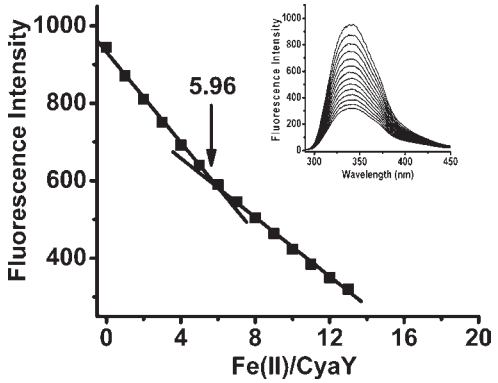

Figure 5. Fluorimetric titration curve of bacterial frataxin CyaY with Fe(II) followed by H_2O_2 titration in increments of 0.2, 0.2 and 0.1 H_2O_2/Fe(II) for a total of 0.5 H_2O_2/Fe(II). Inset: Fluorescence spectra. Conditions: 10 μM CyaY in deoxygenated 50 mM Mops buffer, 150 mM NaCl (pH 7.0) and 25 °C. Each injection corresponds to the anaerobic addition of one Fe(II)/CyaY followed by H_2O_2 titration.

stoichiometry obtained was the same, namely six Fe(III)/CyaY (data not shown).

The initial rate of H^+ production from Fe(II) oxidation by H_2O_2 under anaerobic conditions also reaches a maximum at about six Fe(II)/CyaY as determined by pH-stat measurements (Figure 4). Similarly, anaerobic fluorescence titration of the apoprotein with Fe(II) followed by 0.5 H_2O_2/Fe(II) again showed a discontinuity at about six Fe(II) added per CyaY monomer (Figure 5). Iron analysis of samples containing six Fe(III)/CyaY gave 6.2 (±0.8) Fe(III)/CyaY following centrifugation. Taken together, these observations indicate a binding stoichiometry of six Fe(III)/protein. However, as elaborated below and as evident from the data in Figures 3 and 5, CyaY can accumulate additional iron.

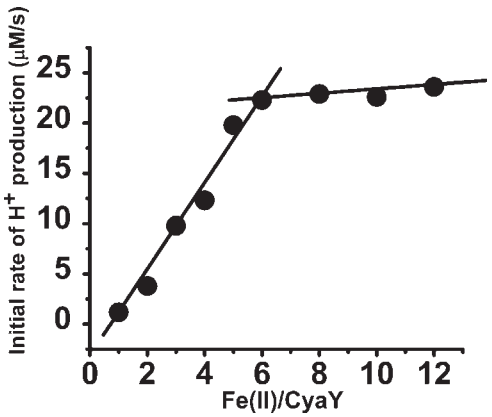

Figure 4. Initial rate of H^+ production *versus* Fe(II)/CyaY ratio for Fe(II) binding and oxidation by H_2O_2 in CyaY under anaerobic conditions. Conditions: 5 μM CyaY in deoxygenated 0.3 mM Mops, 200 mM NaCl (pH 7.5) and 25 °C. Fe(II) was added to the apoprotein solution as 1–4 μl of 1–6 mM $FeSO_4$ stock solution, followed by an excess of hydrogen peroxide (two H_2O_2/Fe(II)). Each point on the graph represents a separate sample.

Fe(II) binding/oxidation: stoichiometries of H^+ production and H_2O_2 consumption

H^+ production during Fe(II) binding

Experiments were carried out to establish the stoichiometric equations for iron binding and oxidation in CyaY. Firstly, to determine whether H^+ is produced upon Fe^{2+} binding to the protein, Fe(II) was added anaerobically to the apoprotein and proton production monitored by autotitration with a standard base (5 mM NaOH) while maintaining the pH at 7.50 with the pH-stat apparatus. Figure 6 shows that ~0.5 H^+/Fe^{2+} is titrated upon the first addition of six Fe(II)/CyaY); this amount corresponds to the free acid in the Fe(II) solution itself as determined by pH stat measurements where Fe(II) is added to the solution in the absence of CyaY. Therefore, we conclude that no protons are produced upon Fe^{2+} binding to the protein at pH 7.5, consistent with the ligands for the Fe(II) being deprotonated at this pH.

Stoichiometry of Fe(II) oxidation by H_2O_2

To determine the stoichiometry of Fe(II) oxidation by H_2O_2, six Fe(II) were added anaerobically to the apoprotein and the solution titrated with H_2O_2 (0.1 H_2O_2/Fe(II) per injection). The spectrophotometric titration showed a discontinuity in absorbance at ~0.5 H_2O_2/Fe(II), indicating that one H_2O_2 oxidizes two Fe(II) (Figure 7, curve B). A 0.5 H_2O_2/Fe(II) stoichiometry was also observed when only two Fe(II)/CyaY (not shown) or 20 Fe(II)/CyaY (Figure 7, curve (A)) were employed. No effect from the ionic strength was observed

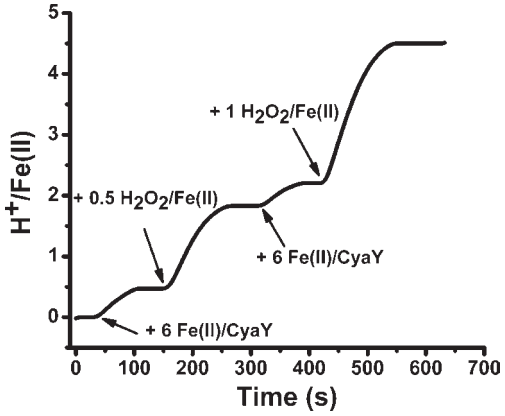

Figure 6. Proton release curve per Fe(II) *versus* time for the indicated amount of Fe(II) and H_2O_2 added to CyaY. Conditions: 5 μM CyaY, 0.3 mM Mops, 200 mM NaCl (pH-stat 7.47), 25 °C; 4.5 μl of 3.33 mM Fe(II) stock solution at pH 3.0 and 1.2 or 2.4 μl of 6.6 mM H_2O_2 in 0.3 mM Mops, 200 mM NaCl (pH 7.47) stock solution were added to the 530 μl protein solution in the pH-stat cell.

when the CyaY experiment was repeated in different media (0.1 M Mops, 50 mM NaCl (pH 7.0 or 7.50), or 50 mM Mops, 200 mM NaCl (pH 7.50)). In a control experiment with egg albumin (six Fe(II)/albumin), titration also gave a H_2O_2/Fe(II) oxidation stoichiometry of 0.5/1 (Figure 7, curve (C)). The formation of polynuclear Fe(III) oxo(hydroxo) species was evident from the UV spectrum of the albumin sample. In a second control experiment with buffer alone, a stoichiometry of 1.03 H_2O_2/Fe(II) was obtained, consistent with the Fenton reaction ($Fe^{2+} + H_2O_2 \rightarrow Fe^{3+} + OH^- + {}^{\cdot}OH$), when 20 μM Fe(II) in 25 mM Mops, 150 mM NaCl (pH 7) was titrated with H_2O_2 in increments of 0.1 H_2O_2/Fe(II).

The anaerobic addition of H_2O_2 (0.5 H_2O_2/Fe(II)) to the six Fe(II)/CyaY sample resulted in the production of 1.50 (±0.15) H^+/Fe(II) ($N = 4$, the number of determinations) from Fe(II) oxidation by H_2O_2 (Figure 6, second addition). In a similar experiment with CyaY, H_2O_2 was added in excess relative to Fe(II) (two H_2O_2/Fe(II)) and again proton production was monitored by autotitration with the standard base. Similar results to those reported in Figure 6 were obtained, confirming the proton count of 1.5 H^+/Fe(II) and the complete oxidation reaction of Fe(II) when H_2O_2 was added at the lower 0.5 H_2O_2/Fe(II) ratio. Accordingly, we write the net reaction for the oxidation of two Fe(II) by a single H_2O_2 in CyaY as follows:

$$2Fe^{2+} + P^Z + H_2O_2 + 2H_2O \rightarrow [(Fe^{3+})_2O(OH)_{3-}P]^{Z+1} + 3H^+ \quad (1)$$

where Z is the charge of the protein and P^Z represents a CyaY monomer.

The molar absorptivity of the observed oxidation product $[(Fe^{3+})_2O(OH)_3 - P]^{Z+1}$ is 1900 (±200) $M^{-1}\,cm^{-1}$ per iron at 296 nm and falls in the range of the molar absorptivities of μ-oxo/hydroxo-bridged iron(III) dimers and small clusters of iron containing proteins and model complexes.[27,28] Similar absorbing species were obtained when O_2 was employed as the oxidant; however, about one hour was required for complete iron oxidation compared to less than 15 s with H_2O_2 as the oxidant (Figure 1(a)).

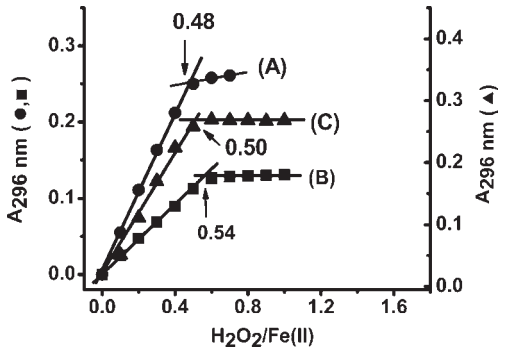

Figure 7. Spectrometric titration curves of CyaY and egg albumin (control) as a function of added hydrogen peroxide for 20 Fe(II)/CyaY (A), six Fe(II)/CyaY (B), six Fe(II)/albumin (C) under argon atmosphere. Conditions: 5 μM CyaY, 100 mM Mops, 50 mM NaCl (pH 7.0) for (A), 10 μM CyaY, 50 mM Mops, 200 mM NaCl (pH 7.50) for (B), and 15 μM egg albumin, 25 mM Mops, 100 mM NaCl (pH 7.0) for (C).

Maximum capacity of iron oxidation and incorporation in CyaY

To determine the maximum amount of iron that the protein can accommodate with H_2O_2 as the oxidant, a spectrophotometric titration was carried out where ten Fe(II)/CyaY were added each time (the first addition being past the six Fe(III)/CyaY endpoint) to the same protein sample followed by incremental additions of H_2O_2 to give a final ratio of 0.5 H_2O_2/Fe(II) for each Fe(II) addition. As shown in Figure 8, a discontinuity in absorbance is seen at about 26 Fe(II)/CyaY suggesting that CyaY can accumulate as many as 26 Fe(III). Precipitation is quite evident beyond 50 Fe(II) added. Analysis of a sample containing 25 Fe(III)/CyaY following centrifugation gave 21.6 (±2.3) Fe(III)/protein, indicating that nearly all of the added iron remains soluble in the presence of the protein when otherwise it would have precipitated as a ferric hydroxide. The molar absorptivity of the oxidized iron species is 2500 (±300) $M^{-1}\,cm^{-1}$ per iron at 296 nm, a value similar to that previously reported for mineralized iron in ferritins.[28–31]

The anaerobic titration of CyaY with Fe(II) produced no discernable changes in the intensity of the intrinsic fluorescence of the protein. However, titration with Fe(II) followed by H_2O_2 each time produced significant quenching of the fluorescence and gave a maximum measured stoichiometry of

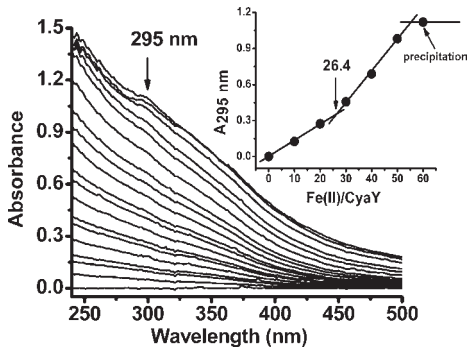

Figure 8. Spectrometric titration spectra of bacterial frataxin CyaY with Fe(II) under anaerobic conditions. Inset: titration curve after the addition of indicated ratios of Fe(II)/protein followed by titration of H_2O_2 for a total of 0.5 H_2O_2/Fe(II). Conditions: 6 μM protein, 50 mM Mops, 200 mM NaCl (pH 7.50).

24 (±1) Fe(III)/CyaY, in accord with the results in Figure 8 (data not shown).

To determine the number of protons produced from the addition of more than six Fe(II) to CyaY with H_2O_2 as the oxidant, a second anerobic addition of six Fe(II)/CyaY was made to the same protein sample already containing six Fe(III)/CyaY (Figure 6, third injection). Again no protons (other than the 0.5 H^+/Fe(II) from the Fe(II) stock solution) were produced. However, upon introduction of H_2O_2 (one H_2O_2/Fe(II)), protons were produced at a ratio of 2.1 (±0.3) H^+/Fe(II) ($N = 3$) (Figure 6, fourth injection). Similar H^+/Fe(II) stoichiometries were obtained from a different set of experiments where 10, 15 or 20 Fe(II)/CyaY were added anaerobically to the protein beyond the initial six Fe(III), followed by enough H_2O_2 to oxidize all the iron present. Thus, the iron oxidation reaction in CyaY beyond the first six irons added to the protein can be written as:

$$2Fe^{2+} + H_2O_2 + 2H_2O \rightarrow 2FeOOH_{(s)} + 4H^+ \quad (2)$$

where FeOOH is an iron oxidized species with UV absorption properties similar to the iron mineral observed with other proteins.[28–31]

Apo-CyaY and holo-CyaY (six Fe(III)/protein) were also examined for catalase activity. An amount of H_2O_2 to give a concentration of 100 μM H_2O_2 was added anaerobically to the 10 μM protein (pH 7.5) solution and the reaction followed for five minutes. Upon addition of H_2O_2, no O_2 evolution was observed as measured by electrode oximetry, a result indicating that neither the apo nor holo proteins exhibit catalase activity. As a control, bovine liver catalase was added to the same solution at the end of the five minute period; O_2 was nearly quantitatively produced, ~95% of that predicted from the disproportionation reaction of H_2O_2 in the presence of catalase ($H_2O_2 \rightarrow H_2O + 1/2O_2$).

EPR spin trapping experiments

Attenuation of hydroxyl radical production

The observed oxidation stoichiometry of two Fe(II) per H_2O_2 suggests that Fenton chemistry which has a 1 : 1 Fe(II)/H_2O_2 stoichiometry should occur minimally in CyaY. In order to determine the ability of the protein to effectively manage the toxicity of Fe^{2+} and H_2O_2, EPR experiments using the spin trap EMPO were performed (Figure 9). All solutions were deoxygenated with argon before each run. Spectrum A of Figure 9 is a control experiment where the addition sequence EMPO + Fe(II) + H_2O_2 in Mops buffer (pH 7.50) was made with H_2O_2 being added incrementally to the solution. As expected from the H_2O_2/Fe(II) oxidation stoichiometry of 1 : 1 noted earlier for buffer, an intense signal from trapped $^{\cdot}OH$ radical is observed (curve A). A second control experiment with the addition sequence albumin + EMPO + Fe(II) + H_2O_2 (six Fe(II)/albumin) in the same buffer is represented in spectrum B. Again an intense EPR spectrum is seen even though the net H_2O_2/Fe(II) stoichiometry is 0.5 for this protein (Figure 7, curve C). This result implies that Fe(II) oxidation by H_2O_2 in the presence of albumin occurs by a two-step process where the $^{\cdot}OH$ produced in equation (3) below is trapped through reaction with EMPO (25 mM) before it can react with the additional Fe(II) (96 μM) by equation (4) to give

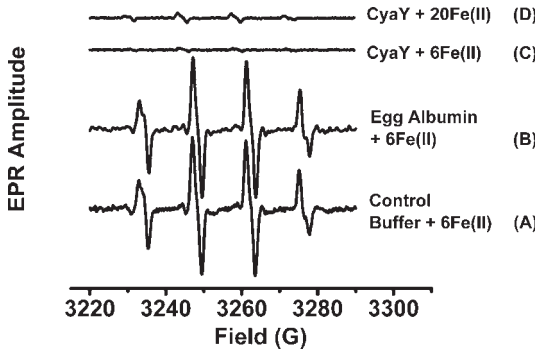

Figure 9. X-band EPR signal of EMPO-OH adduct in 50 mM Mops, 200 mM NaCl (pH 7.50) (A). Anaerobic addition sequence EMPO + Fe(II) + H_2O_2; (B) anaerobic addition sequence egg albumin + EMPO + Fe(II) + H_2O_2; (C) anaerobic addition sequence apo-CyaY + EMPO + six Fe(II)/protein + H_2O_2; (D) anaerobic addition sequence apo-CyaY + EMPO + 20 Fe(II)/protein + H_2O_2. Conditions: 16.6 μM CyaY or 13.8 μM egg albumin, 25 mM EMPO, H_2O_2 was titrated in small increments of (0.06–0.1) H_2O_2/Fe(II) until a ratio of 1.0–1.2 H_2O_2/Fe(II) was reached. The time interval between H_2O_2 additions was typically 30–40 seconds and the sample was ready for EPR measurement in less than ten minutes. Typical spectrometer parameters were: microwave power 5.0 mW, modulation amplitude 0.5 G, time constant 0.163 second, scan rate 0.834 G s^{-1}, signal averaged 4X (spectra A and B) and time constant 1.0 seconds, scan rate 0.07 G s^{-1}, single scan (spectra C and D). Room temperature.

the net reaction of equation (5):

$$Fe^{2+} + H_2O_2 \rightarrow Fe^{3+} + OH^- + {}^{\cdot}OH \quad (3)$$

$$Fe^{2+} + {}^{\cdot}OH \rightarrow Fe^{3+} + OH^- \quad (4)$$

$$2Fe^{2+} + H_2O_2 \rightarrow 2Fe^{3+} + 2OH^- \quad (5)$$

In contrast to buffer (spectrum (A)) and albumin (spectrum (B)), hydroxyl radical production is significantly attenuated in the presence of CyaY. Spectra (C) and (D) correspond to the addition sequences CyaY + EMPO + 6 or 20 Fe(II)/CyaY + H_2O_2, respectively. Little hydroxyl radical is trapped (2.6% and 7.2% of that in curve (A), respectively). These spin trapping results plus the measured 0.5 H_2O_2/Fe(II) stoichiometry for CyaY (Figure 7, curves (A) and (B)) suggest that Fe(II) is oxidized by H_2O_2 in a single pair-wise step in this protein as described by equation (1). However, when H_2O_2 is added to the CyaY prior to the addition of Fe(II), an oxidation stoichiometry 1 : 1 H_2O_2/Fe(II) is observed and an intense EPR spectrum is obtained (not shown). In this instance, the Fe(II) presumably reacts directly with the H_2O_2 in the solution before the Fe(II) has sufficient time to bind to the protein, resulting in a loss of the protective effect of CyaY against iron induced radical formation.

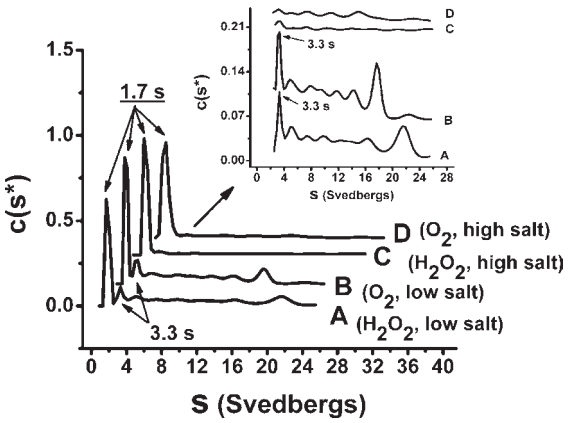

Figure 10. Sedimentation coefficient distribution $c(s^*)$ *versus* s, for CyaY. A and C, CyaY + Fe(II) + H_2O_2. B, and D, CyaY + Fe(II) + O_2. The inset illustrates on an expanded scale the aggregate species present. Conditions: 25 μM CyaY, 150 μM Fe(II), samples A and B were in 20 mM Hepes, 10 mM NaCl (pH 7.0) and samples C and D were in 50 mM Hepes, 150 mM NaCl (pH 7.0), 20 °C, 280 nm, 45,000 rpm. Fe(II) was added in increments of two Fe(II)/CyaY and titrated with H_2O_2 in increments of 0.1 H_2O_2/Fe(II) until a ratio of 0.5 H_2O_2/Fe(II) was reached. When O_2 was the oxidant, additions of Fe(II) were spaced 30–45 minutes to ensure complete oxidation.

Sedimentation equilibrium and velocity measurements

Yeast frataxin has been shown to assemble into a large aggregate in the presence of iron, forming a shell-like structure encapsulating an iron mineral core.[25] Ultracentrifugation experiments were therefore carried out on CyaY to establish whether the bacterial protein exhibits similar assembly properties. Sedimentation velocity measurements with the protein in the absence of iron showed a single component at $s \sim 1.7$ (±0.2) corresponding to a molecular mass of 12,500 (±500) Da. This value was confirmed by sedimentation equilibrium measurements and is in accord with the protein being monomeric in solution in the absence of iron.

The addition of iron (six Fe(II)/CyaY in 21% O_2 or anaerobically followed by H_2O_2 titration) caused the formation of multiple components in the sedimentation velocity profile of the sample (Figure 10). Higher iron additions (up to 40 Fe(II)/CyaY) did not change the species distribution profile from that shown in Figure 10 and both O_2 and H_2O_2 promoted similar assembly patterns. However, the ionic strength of the solution had a pronounced effect on the amount of protein aggregation observed (Figure 10, curves A and B *versus* C and D). More protein aggregation, 60–70% of the total, was obtained when a low salt concentration was used as shown in curves A and B (10 mM NaCl or KCl) compared to only 20–30% when a higher salt concentration was employed as shown in curves C and D (150 mM NaCl or KCl) (Figure 10). Significantly, sedimentation velocity measurements with egg albumin (six Fe(III)/protein followed by H_2O_2 titration) as a control under similar conditions as described for Figure 10 likewise showed the formation of multiple high molecular mass assemblies as seen with CyaY (data not shown).

To determine whether the formation of disulfide bridges from exposed cysteine residues (Cys32 and Cys80) might be responsible for the aggregation observed with Fe(II) and H_2O_2, CyaY was first alkylated with excess iodoacetamide (IAA) in 50 mM Mops, 150 mM NaCl (pH 7.0) at room temperature ([IAA]/[CyaY] = 10 for four hours) followed by the anaerobic addition of six Fe(II) to CyaY and then H_2O_2. A similar percentage of aggregation (33% of total protein) to that seen in Figure 10 in the absence of iodoacetamide was observed. Therefore, the cysteine residues do not appear to be significantly involved in cross-linking of the protein.

The effect of adding Fe(II) or H_2O_2 alone to CyaY in promoting protein aggregation was also examined by sedimentation velocity measurements. When H_2O_2 was added to the apoprotein in a 10 : 1 ratio, no protein aggregation was seen, indicating that H_2O_2 itself is not responsible for the observed aggregation. However, when the apoprotein was incubated overnight with ten Fe(II)/CyaY under anaerobic conditions and in the presence of 10 mM sodium dithionite ($Na_2S_2O_4$) in 50 mM Mops, 150 mM NaCl (pH 7.0), a sedimentation pattern quite unlike that in Figure 10 was observed. The monomeric 1.7 S (M_r 12,500) apoprotein

species was replaced over time by a species of M_r 47,200 (4.22 S), corresponding to a tetramer (results not shown).

The aggregation induced by addition of metal ions Fe(II) and Fe(III), and also Ca(II) (not shown), was readily reversed by the addition of chelating agents such as EDTA or EGTA. This result is a further indication that covalent cross-linking of the protein is not responsible for the observed association. Thus, protein aggregation appears to be a consequence of metal ion binding simultaneously to multiple subunits in some type of bridging fashion.

Discussion

We have carried out here a detailed characterization of the iron binding and kinetic properties of CyaY. Since it has been suggested that frataxins have ferritin-like activity it is appropriate to compare our findings with those obtained for ferritin. Bacterial frataxin CyaY exhibits similar iron oxidation and detoxification properties to those of the heme-containing bacterioferritin (EcBFR) and the DNA binding protein from starved cells (Dps).[27,28] However, unlike EcBFR but similar to Dps, O_2 is a poor oxidant for Fe(II) in CyaY (Figure 1), indicating that CyaY lacks ferroxidase activity with O_2. When H_2O_2 is used as the Fe(II) oxidant, rapid and complete oxidation of Fe(II) is observed (Figure 1(a), curve (A)) with a stoichiometry of two Fe(II) per H_2O_2 (Figure 7, curves (A) and (B)). The fastest rate of oxidation with H_2O_2, which is not catalytic, is achieved once six or more Fe(II) have been cumulatively added to the protein (Figure 1(b)). The associated binding and oxidation of Fe(II) in CyaY causes an increase in absorbance at 295–305 nm from polynuclear Fe(III) hydroxo(oxo) species (Figures 1 and 3) where the Fe(III) remains solubilized with the protein, unlike the situation in buffer alone where ferric hydroxide precipitation occurs (Figure 1, curves (C) and (D)).

Pair-wise oxidation of Fe(II) by H_2O_2 in CyaY (equations (1) and (2)) avoids the production of hydroxyl radicals and the damaging effect of these highly reactive species. Similar oxidation reactions have been observed with *E. coli* bacterioferritin and Dps.[27,28] Consistent with equations (1) and (2), the spin trapping experiments (Figure 9) show that hydroxyl radical production is greatly attenuated in the presence of CyaY at all levels of Fe(II) added. The ability of CyaY to facilitate pair-wise oxidation of Fe(II) by H_2O_2 is probably due to the presence of a dinuclear iron binding site on this protein that is absent on albumin but found on known iron binding and detoxification proteins.[26–31] The attenuating effect of CyaY on hydroxyl radical production is in agreement with recent studies suggesting that increased oxidative damage and iron induced formation of free radicals are associated with deficiency in frataxin.[19,32–34]

ITC titration of CyaY with Fe(II) anaerobically reveals an exothermic event ($\Delta H^\circ = -4.88$ kJ/mol) with a binding stoichiometry of two ferrous ions per frataxin monomer (Figure 2). The relatively large positive entropy ($\Delta S^\circ = 87.20$ J/mol K) of binding indicates that the interaction of Fe(II) with CyaY is largely entropically driven, as previously observed for the binding of Fe(II), Zn(II) and Tb(III) to human ferritins.[35,36] The significant entropy change observed is presumably due to the changes in the hydration of the protein and of the metal ion upon binding to the protein. The ITC data indicate that at least two Fe(II) relatively weakly associate with CyaY ($K_D \sim 4$ μM) and are thus bio-available. Based on the facile iron binding and displacement, one interpretation is that CyaY may act as mitochondrial iron chaperon that prevents the participation of iron in Fenton chemistry while keeping it available for different biosynthetic pathways as suggested for yeast and human frataxins.[12,16,23–25]

Kinetic, spectrophotometric and spectrofluorimetric titrations and pH-stat measurements of Fe(II) binding and oxidation in CyaY using H_2O_2 as oxidant all show a stoichiometry of six Fe(III)/CyaY (Figures 1(b), and 3–5) as does human frataxin,[23] implying that a minimum of six Fe(III) per monomer are produced in the first stage of iron oxidation, ultimately leading to the sequestration of as many as 26 Fe(III) atoms per monomer (Figure 8). Two of the six Fe(III) are probably derived from oxidation of the two bound Fe(II) observed by ITC. The other four Fe(III) may be produced as a result of cluster formation or from Fe(II) oxidation at additional weaker Fe(II) binding sites suggested by the ultrafiltration experiment. The kinetic data showing a minimum half-life for iron oxidation once six Fe(II) have been added to the protein (Figure 1(b)) suggests a change in mechanism, perhaps to one no longer involving the protein binding sites. At this stage, further iron oxidation probably occurs directly on the surface of a preformed cluster of Fe(III) associated with the protein or on the highly anionic and conserved surface of the protein.[26]

The oxidation reaction of Fe(II) by H_2O_2 in CyaY (equation (1)) is similar to that found for Dps,[27] in that both of them produce the same number of protons with the same Fe(II)/H_2O_2 oxidation stoichiometry of 2/1. The Fe(II) oxidation reaction beyond six Fe(II)/CyaY (equation(2)) is identical to other iron mineralization protein reactions where H_2O_2 again oxidizes Fe(II) pair-wise with the production of two H^+ per Fe(II) oxidized.[27,28] The fact that the H^+/Fe(II) stoichiometry and the rates of proton release are different for the first and second additions of six Fe(II)/CyaY (Figures 4 and 6) is a further indication of a change in reaction mechanism beyond the first six irons added.

Unlike yeast frataxin,[25] the bacterial protein CyaY does not assemble into a predominantly single high molecular mass species holding large amounts of iron(III) inside its protein shell as found in ferritins. Instead, only partial aggregation

occurs with Fe(III), forming several species but none in great abundance (Figure 10). In the absence of metal ions, CyaY exists as a monomer in solution. The sensitivity of the Fe(III) induced aggregated species to salt concentration and the fact that albumin also aggregates in the presence of six Fe(III)/albumin strongly suggests that the observed Fe(III) induced assembly is a non-specific effect that is probably not relevant to the function of CyaY.

Studies on *Saccharomyces cerevisiae* and mammalian cells have concluded that frataxin is a conserved mitochondrial protein required for iron homeostasis.[8,9,32,37,38] Several previous observations support the hypothesis that mitochondrial iron accumulation, hypersensitivity to oxidative stress, and inadequate iron–sulfur cluster synthesis occur in Friedreich's ataxia, a consequence of frataxin deficiency.[12]Yeast frataxin may have an iron storage function presumably because it does not have a mitochondrial ferritin as found in humans. Human frataxin may have lost the storage function, primarily serving as a mitochondrial iron chaperon and helping to prevent the Fenton reaction, as suggested by the present work with CyaY, while keeping iron available for biosynthetic pathways. Consistent with this idea, is the report that human frataxin binds approximately six ferrous or ferric ions per monomer and delivers them for the biosynthesis of Fe–S clusters[23] and heme[24,25] inside the mitochondria. CyaY may act like human frataxin by binding ferrous iron and keeping it available for these iron biosynthetic processes. The bacterial protein CyaY may also work synergistically with other chaperon proteins by signaling and assisting the synthesis of iron–sulfur cluster biogenesis. This hypothesis is supported by the recent observation that bacterial frataxin is genetically linked with two known iron–sulfur cluster assembly chaperon proteins, HSP66 and HSP20.[39] If this picture turns out to be at least partially true, it would therefore indicate that bacterial frataxin may act as a sensor for mitochondrial iron status through which the mechanism of iron–sulfur cluster assembly is regulated. Mitochondrial iron overload, impaired iron–sulfur cluster and oxidative damage would otherwise be the direct consequences of frataxin deficiency.

In conclusion, the present study has defined much of the iron chemistry of the bacterial frataxin, CyaY. The *in vitro* data presented here suggest that frataxin may help to prevent iron-induced oxidative damage while maintaining the iron pool within the mitochondria in a soluble, non-toxic and bio-available form for biosynthetic pathways. Consistent with this hypothesis, a proposed model of frataxin function inside the mitochondria suggests that frataxin deficiency would promote immediate oxidative damage followed by progressive iron accumulation.[2] The sequence of these events may explain the early embryonic lethality induced by deletion of the mouse frataxin gene before detectable levels of iron can accumulate.[40]

Materials and Methods

The recombinant CyaY was expressed in *E. coli* and purified in the iron-free form as described[26] and the protein concentration was determined from its absorbance at 280 nm using a molar absorptivity of 29,970 $M^{-1}\,cm^{-1}$. Chicken egg albumin was obtained from Sigma-Aldrich. All chemicals were of reagent grade quality and used without further purification. The freshly prepared stock solutions of hydrogen peroxide were assayed by electrode oximetry from the amount of O_2 produced upon addition of catalase (EC 1.11.1.6; 65,000 units/mg; Roche Molecular Biochemicals) or from its absorbance at 240 nm ($\epsilon = 43.6\ M^{-1}\,cm^{-1}$).[29] The 5-ethoxycarbonyl-5-methyl-1-pyrroline-*N*-oxide (EMPO) spin trap was purchased from Oxis Research (Portland, OR), diethylenetriamine pentaacetic acid (DTPA) from Sigma, and iodoacetaminde (IAA) from Aldrich, EDTA from Pierce, and EGTA from J. T. Baker.

The oximetry/pH-stat apparatus was standardized and operated as described.[30,31] All the solutions were thoroughly deoxygenated by purging with high purity grade argon gas (99.995%; <5 ppm O_2) before experiments involving the anaerobic oxidation of Fe(II) by H_2O_2. In the pH-stat experiments, the use of 0.3 mM 3-(*N*-morpholino)propane-sulfonic acid (Mops) buffer increased the stability of the pH-stat control without significantly buffering the solution. Background compensations for the free acid in the ferrous sulfate stock solutions were made in all calculations.

The ultraviolet–visible difference spectrophotometric titrations and kinetic measurements of Fe(II) oxidation by H_2O_2 or O_2 in CyaY were performed on a Cary 50 spectrophotometer. For the anaerobic experiments, 1 ml of deoxygenated apo-CyaY solution was added to a quartz cuvette maintained under constant positive atmosphere of pure argon through a septum in the cuvette cap. The instrument was zeroed with the apoprotein alone in the same buffer solution prior to all absorbance measurements. In the kinetic measurements of Fe(II) oxidation by O_2, Ferrozine was used to quench the reaction and the concentration of unreacted Fe(II) measured from the absorbance of the Fe(II)$(Ferrozine)_3$ complex at 562 nm using $\varepsilon = 27{,}900\ M^{-1}\,cm^{-1}$.[42]

The spin-trapping EPR experiments were measured on a laboratory assembled EPR spectrophotometer as described elsewhere[27] or on a Bruker EleXsys E-500 EPR spectrometer. The responses of the two instruments were calibrated to one another by running the same spin trapped radical sample on each. All spectra were recorded immediately after the addition of the last reagent. The conditions of the experiment and the parameters of the spectrometer are indicated in the legend to Figure 9.

Sedimentation velocity measurements were carried out on a Beckman XLI analytical ultracentrifuge using either absorbance or interference optics. The experiments were conducted at different rotor speeds (12,000–60,000 rpm) at 20 °C with a protein concentration between 20 and 55 μM. Radial absorbance scans were collected at both 280 nm and 310 nm using the continuous scanning mode to provide an effective radial resolution of 30 μm. Plots of $c(s^*)$ *versus* s were obtained using the observed sedimentation data and Lamm equation as described.[41]

The iron content of protein samples was carried out spectrophotometrically using the Ferrozine assay after first reducing Fe(III) to Fe(II) with ascorbate in trichloroacetic acid.[42]

Fluorescence measurements were performed at room temperature in 50 mM Mops, 150 mM NaCl (pH 7.52), on a Varian Cary Eclipse fluorimeter with excitation at 280 nm. The bandwidths of the excitation and emission monochromators were 5 nm.

Isothermal titration calorimetry (ITC) measurements of Fe(II) binding were carried out at 25.00 °C with an upgraded CSC model 4200 isothermal calorimeter (Calorimetry Science Corporation, Provo, Utah). The instrument operation and calibration were performed as described.[35,36] All the thermodynamic parameters including the standard enthalpy change (ΔH^o), the binding constant (K) and the stoichiometry of binding (n) were determined from a single ITC experiment. From these experimental values, the standard entropy change (ΔS^o) and the standard Gibbs free energy change (ΔG^o) were calculated, $\Delta G^o = -RT \ln K$, and $\Delta S^o = (\Delta H^o - \Delta G^o)/T$, respectively. Curve fitting was done with BindWorks 3.0 software (Calorimetry Sciences Corp.) using a model for multiple Fe(II) ions independently binding to a single CyaY monomer. Although the ultracentrifugation experiments revealed that protein aggregation occurs upon Fe(II) binding, the above model fits the ITC data quite well. Experimental conditions are given in the Figure legends.

Ultrafiltration studies of Fe(II) binding were carried out with a 3 ml Amicon cell fitted with a YM 3 membrane. Microliter increments of 2–5 mM $FeSO_4$ solution were added to 2 ml of deoxygenated 8–10 μM CyaY in 50 mM Mops, 150 mM NaCl (pH 7.0) and the volume reduced under Ar pressure to 1 ml each time followed by the addition of 1 ml of deoxygenated buffer plus additional $FeSO_4$ in the presence of 2–5 mM dithionite ($Na_2S_2O_4$). The Fe(II) content of the 1 ml of ultrafiltrate following each addition of increasing amounts of Fe(II) to the cell was measured using either the bathophenantroline–disulfonic acid (BPS, 22,140 M^{-1} cm^{-1} at 535 nm) or the Ferrozine assay.[43] A control experiment in the absence of protein demonstrated that the membrane did not bind or retain Fe(II) in the cell.

Acknowledgements

The authors thank Dr Meihong Su for performing some of the control experiments and Ms Kari Hartman for making the analytical ultracentrifugation measurements.

This work was supported by grant R01 GM20194 from the National Institute of General Medical Sciences (to N.D.C.), by Seek a Miracle/MDA and the Friedreich Ataxia Research Alliance (FARA) foundations (to A.P.) and by grant NSF DBI 9876582 from the National Science Foundation (to T.M.L.).

References

1. Muhlenhoff, U. & Lill, R. (2000). Biogenesis of iron–sulfur proteins in eukaryotes: a novel task of mitochondria that is inherited from bacteria. *Biochim. Biophys. Acta*, **1459**, 370–382.
2. Patel, P. I. & Isaya, G. (2001). Friedrich's ataxia: from GAA triplet-repeat expansion to frataxin deficiency. *Am. J. Hum. Genet.* **69**, 15–24.
3. Flatmark, T. & Romslo, I. (1975). Energy-dependent accumulation of iron by isolated rat liver mitochondria. Requirement of reducing equivalents and evidence for a unidirectional flux of Fe(II) across the inner membrane. *J. Biol. Chem.* **250**, 6433–6438.
4. Kispal, G., Csere, P., Guiard, B. & Lill, R. (1997). The ABC transporter Atm1p is required for mitochondrial iron homeostasis. *FEBS Letters*, **418**, 346–350.
5. Knight, S. A. B., Sepuri, N. B. V., Pain, D. & Dancis, A. (1998). Mt-Hsp70 homolog, Ssc2p, required for maturation of yeast frataxin and mitochondrial iron homeostasis. *J. Biol. Chem.* **273**, 18389–18393.
6. Lange, H., Kispal, G. & Lill, R. (1999). Mechanism of iron transport to the site of heme synthesis inside yeast mitochondria. *J. Biol. Chem.* **274**, 18989–18996.
7. Gibson, T. J., Koonin, E. V., Musco, G., Pastore, A. & Bork, P. (1996). Friedreich's ataxia protein: phylogenetic evidence for mitochondrial dysfunction. *Trends Neurosci.* **19**, 465–468.
8. Cavadini, P., Gellera, C., Patel, P. I. & Isaya, G. (2000). Human frataxin maintains mitochondrial iron homeostasis in *Saccharomyces cerevisiae*. *Hum. Mol. Genet.* **9**, 2523–2530.
9. Radisky, D. C., Babcock, M. C. & Kaplan, J. (1999). The yeast frataxin homologue mediates mitochondrial iron efflux. Evidence for a mitochondrial iron cycle. *J. Biol. Chem.* **274**, 4497–4499.
10. Wong, A., Yang, J., Cavadini, P., Gellera, C., Lonnerdal, B., Taroni, F. & Cortopassi, G. (1999). The Friedreich's ataxia mutation confers cellular sensitivity to oxidant stress which is rescued by chelators of iron and calcium and inhibitors of apoptosis. *Hum. Mol. Genet.* **8**, 425–430.
11. Campuzano, V., Montermini, L., Molto, M. D., Pianese, L., Cossee, M., Cavalcanti, F. *et al.* (1996). Friedreich's ataxia: autosomal recessive disease caused by an intronic GAA triplet repeat expansion. *Science*, **271**, 1423–1427.
12. Pandolfo, M. (2002). Iron metabolism and mitochondrial abnormalities in Friedreich ataxia. *Blood Cells Mol. Dis.* **29**, 536–547.
13. Koutnikova, H., Campuzano, V., Foury, F., Dolle, P., Cazzalini, O. & Koenig, M. (1997). Studies of human, mouse and yeast homologues indicate a mitochondrial function for frataxin. *Nature Genet.* **16**, 345–351.
14. Becker, E. & Richardson, D. R. (2001). Frataxin: its role in iron metabolism and the pathogenesis of Friedreich's ataxia. *Int. J. Biochem. Cell Biol.* **33**, 1–10.
15. Park, S., Gakh, O., Mooney, S. M. & Isaya, G. (2002). The ferroxidase activity of yeast frataxin. *J. Biol. Chem.* **277**, 38589–38595.
16. Cavadini, P., O'Neill, H. A., Benada, O. & Isaya, G. (2002). Assembly and iron-binding properties of human frataxin, the protein deficient in Friedreich ataxia. *Hum. Mol. Genet.* **11**, 217–227.
17. Nichol, H., Gakh, O., O'Neill, H. A., Pickering, I. J., Isaya, G. & George, G. N. (2003). Structure of frataxin iron cores: an x-ray absorption spectroscopic study. *Biochemistry*, **42**, 5971–5976.
18. Gakh, O., Adamec, J., Gacy, A. M., Twesten, R. D., Owen, W. G. & Isaya, G. (2002). Physical evidence that yeast frataxin is an iron storage protein. *Biochemistry*, **41**, 6798–6804.
19. Adamec, J., Rusnak, F., Owen, W. G., Naylor, S., Benson, L. M., Gacy, A. M. & Isaya, G. (2000). Iron-dependent self-assembly of recombinant yeast frataxin: implications for Friedreich ataxia. *Am. J. Hum. Genet.* **67**, 549–562.

20. Ramazzotti, A., Vanmansart, V. & Foury, F. (2004). Mitochondrial functional interactions between frataxin and Isu1p, the iron–sulfur cluster scaffold protein, in *Saccharomyces cerevisiae*. *FEBS Letters*, **557**, 215–220.
21. Duby, G., Foury, F., Ramazzotti, A., Herrmann, J. & Lutz, T. (2002). A non-essential function for yeast frataxin in iron–sulfur cluster assembly. *Hum. Mol. Genet.* **11**, 2635–2643.
22. Gerber, J., Muehlenhoff, U. & Lill, R. (2003). An interaction between frataxin and Isu1/Nfs1 that is crucial for Fe/S cluster synthesis on Isu1. *EMBO Reports*, **4**, 906–911.
23. Yoon, T. & Cowan, J. A. (2003). Iron–sulfur cluster biosynthesis. Characterization of Frataxin as an iron donor for assembly of [2Fe-2S] clusters in ISU-type proteins. *J. Am. Chem. Soc.* **125**, 6078–6084.
24. Yoon, T. & Cowan, J. A. (2004). Frataxin-mediated iron delivery to ferrochelatase is the final step of heme biosynthesis. *J. Biol. Chem.* **279**, 25943–25946.
25. Park, S., Gakh, O., O'Neill, H. A., Mangravita, A., Nichol, H., Ferreira, J. C. & Isaya, G. (2003). Yeast frataxin sequentially chaperones and stores iron by coupling protein assembly with iron oxidation. *J. Biol. Chem.* **278**, 31340–31351.
26. Adinolfi, S., Trifuoggi, M., Politou, A., Martin, S. & Pastore, A. (2002). A structural approach to understanding the iron-binding properties of phylogenetically different frataxins. *Hum. Mol. Genet.* **11**, 1865–1877.
27. Zhao, G., Ceci, P., Ilari, A., Giangiacomo, L., Laue, T. M., Chiancone, E. & Chasteen, N. D. (2002). Iron and hydrogen peroxide detoxification properties of DNA-binding protein from starved cells: a ferritin-like DNA-binding protein of *Escherichia coli*. *J. Biol. Chem.* **277**, 27689–27696.
28. Bou-Abdallah, F., Lewin, A. C., Le Brun, N. E., Moore, G. R. & Chasteen, N. D. (2002). Iron detoxification properties of *Escherichia coli* bacterioferritin. *J. Biol. Chem.* **277**, 37064–37069.
29. Zhao, G., Bou-Abdallah, F., Yang, X., Arosio, P. & Chasteen, N. D. (2001). Is hydrogen peroxide produced during iron(II) oxidation in mammalian apoferritins? *Biochemistry*, **40**, 10832–10838.
30. Yang, X., Le brun, N. E., Thomson, A. J., Moore, G. R. & Chasteen, N. D. (2000). The iron oxidation and hydrolysis chemistry of *Escherichia coli* bacterioferritin. *Biochemistry*, **39**, 4915–4923.
31. Yang, X., Chen-Barrett, Y., Arosio, P. & Chasteen, N. D. (1998). Reaction paths of iron oxidation and hydrolysis in horse spleen and recombinant human ferritins. *Biochemistry*, **37**, 9743–9750.
32. Babcock, M., de silva, D., Oaks, R., Davis-Kaplan, S., Jiralerspong, S., Montermini, L. *et al.* (1997). Regulation of mitochondrial iron accumulation by Yfh1p, a putative homolog of frataxin. *Science*, **276**, 1709–1712.
33. Karthikeyan, G., Santos, J. H., Graziewicz, M. A., Copeland, W. C., Isaya, G., Van Houten, B. & Resnick, M. A. (2003). Reduction in frataxin causes progressive accumulation of mitochondrial damage. *Hum. Mol. Genet.* **12**, 3331–3342.
34. Karthikeyan, G., Lewis, L. K. & Resnick, M. A. (2002). The mitochondrial protein frataxin prevents nuclear damage. *Hum. Mol. Genet.* **11**, 1351–1362.
35. Bou-Abdallah, F., Arosio, P., Santambrogio, P., Yang, X., Janus-Chandler, C. & Chasteen, N. D. (2002). Ferrous ion binding to recombinant human H-chain ferritin. An isothermal titration calorimetry study. *Biochemistry*, **41**, 11184–11191.
36. Bou-Abdallah, F., Arosio, P., Levi, S., Janus-Chandler, C. & Chasteen, N. D. (2003). Defining metal ion inhibitor interactions with recombinant human H- and L-chain ferritins and site-directed variants: an isothermal titration calorimetry study. *J. Biol. Inorg. Chem.* **8**, 489–497.
37. Foury, F. & Talibi, D. (2001). Mitochondrial control of iron homeostasis. A genome wide analysis of gene expression in a yeast frataxin-deficient strain. *J. Biol. Chem.* **276**, 7762–7768.
38. Branda, S. S., Yang, Z. Y., Chew, A. & Isaya, G. (1999). Mitochondrial intermediate peptidase and the yeast frataxin homolog together maintain mitochondrial iron homeostasis in *Saccharomyces cerevisiae*. *Hum. Mol. Genet.* **8**, 1099–1110.
39. Huynen, M. A., Snel, B., Bork, P. & Gibson, T. J. (2001). The phylogenetic distribution of frataxin indicates a role in iron–sulfur cluster protein assembly. *Hum. Mol. Genet.* **10**, 2463–2468.
40. Cossee, M., Puccio, H., Gansmuller, A., Koutnikova, H., Dierich, A., LeMeur, M. *et al.* (2000). Inactivation of the Friedreich ataxia mouse gene leads to early embryonic lethality without iron accumulation. *Hum. Mol. Genet.* **9**, 1219–1226.
41. Schuck, P., Perugini, M. A., Gonzales, N. R., Howlett, G. J. & Schubert, D. (2002). Size-distribution analysis of proteins by analytical ultracentrifugation: strategies and application to model systems. *Biophys. J.* **82**, 1096–1111.
42. Percival, M. D. (1991). Human 5-lipoxygenase contains an essential iron. *J. Biol. Chem.* **266**, 10058–10061.
43. Cowart, R. E., Singleton, F. L. & Hind, J. S. (1993). A comparison of bathophenanthroline-disulfonic acid and Ferrozine as chelators of iron(II) in reduction reactions. *Anal. Biochem.* **211**, 151–155.

Edited by R. Huber

(Received 9 January 2004; received in revised form 25 May 2004; accepted 27 May 2004)